A high-throughput contact-hole resolution metric for photoresists: full-process sensitivity study

Christopher N. Anderson[a] and Patrick P. Naulleau[b]

[a]Applied Science & Technology Graduate Group, University of California, Berkeley
Berkeley, CA 94720, USA;
[b]Center for X-ray Optics, Lawrence Berkeley National Laboratory
1 Cyclotron Road, Berkeley, CA 94720, USA

ABSTRACT

The ability to accurately quantify the intrinsic resolution of chemically amplified photoresists is critical for the optimization of resists for extreme ultraviolet (EUV) lithography. We have recently reported on two resolution metrics that have been shown to extract resolution numbers consistent with direct observation. In this paper we examine the previously reported contact-hole resolution metric and explore the sensitivity of the metric to potential error sources associated with the experimental side of the resolution extraction process. For EUV exposures at the SEMATECH Berkeley microfield exposure tool, we report a full-process error-bar in extracted resolution of 1.75 nm RMS and verify this result experimentally.

Keywords: Extreme ultraviolet, EUV, lithography, resolution, photoresist

1. INTRODUCTION

Extreme ultraviolet (EUV) lithography continues to be the leading candidate for high-volume chip production beyond the 32-nm technology node and has now entered the commercialization phase.[1,2] One of the biggest challenges still facing EUV is the development of resists that simultaneously achieve the resolution, sensitivity and line-edge-roughness (LER) requirements for commercialization.[3,4] A large part of the resist development task relies on print-based performance tests to identify resist formulations that meet the demanding specs beyond the 32-nm node. Resist sensitivity and LER are easy to quantify and compare based on direct observation of printing results. The determination of intrinsic resolution, however, is less straightforward.

To address the issue of intrinsic resolution quantification, a variety of methods have been developed including the iso-focal bias,[5] LER correlation length,[6] modulation transfer function (MTF),[7,8] and contact-hole[9] resolution metrics. Of these four metrics, it has been shown that only the MTF and contact-hole metrics extract resolutions that are consistent with direct observation.[9,10] At the present time, the contact-hole resolution metric is the most attractive candidate for high-throughput resist screening owing to the fact that it is the most efficient*.[9]

In previous work the error-bars of the contact-hole metric have been determined at EUV wavelengths based on known uncertainties in exposure tool aberrations and focus control that limit the ability to accurately model the aerial image at the wafer surface in an exposure.[9] In this paper we characterize the sensitivity of the contact-hole metric to potential error sources associated with the experimental side of the resolution extraction process. We will explore the following issues: picking the best-focused row from a focus-exposure matrix (FEM), scanning electron microscope (SEM) focus, SEM electron beam dosing, and SEM image analysis. We also perform a full-process reproducibility study to observe how the entire process holds up against the collection of experimental and modeling errors.

Further author information: (Send correspondence to C.N.A.)
C.N.A: E-mail: cnanderson@berkeley.edu, Telephone: 1 510 486 5288
P.P.N.: E-mail: pnaulleau@lbl.gov, Telephone: 1 510 486 4529

*Efficiency is determined by the number of exposure tool use-hours, SEM images, analysis time and modeling support required for resolution extraction, with less time and effort being more efficient.

2. THE CONTACT-HOLE RESOLUTION METRIC

The contact-hole resolution metric has been described in detail in the literature.[9] In summary, it involves measuring the printed diameter (PD) of contact-holes through dose at or near nominal focus and comparing the experimental PD vs. dose data to modeled PD vs. dose data at nominal focus for varying degrees of resist blur assuming the PSF-blur model.[11] Resolution (blur) is extracted by finding the PSF-blur that minimizes the mean-squared-error between the modeled PD vs. dose curve experimental PD vs. dose data.

Typically the resolution extraction process begins by capturing SEM images of printed contact-holes through dose. Each SEM image is then analyzed by software to compute the average and variance of the contact-hole PD and LER. These data, combined with dose information from printing, are used to produce a PD vs. dose curve that is curve-fit to find the dose-to-size[†] dose. All absolute dose data is then normalized by the dose-to-size dose to enable cross-platform comparisons. Each step in this process leads to potential sources of error that will be explored in this work to determine how they affect the resulting extraction.

All experimental data we present is obtained at the SEMATECH Berkeley MET EUV printing facility with $\sigma = 0.35 - 0.55$ annular pupil fill.[12] All contact-hole features are dark-field (the contact is bright in the aerial image) and are coded to print with a 50 nm diameter and 125 nm pitch (1:1.5 duty cycle). In previous work the error-bars on extracted resolution, as determined by aerial-image modeling limitations due to uncertainty in exposure tool aberrations and focus control at the Berkeley facility, were reported at 3.32 nm peak-to-valley and 1.23 nm RMS[9]

3. PICKING THE BEST-FOCUS ROW IN A FEM

To ensure each wafer has one set of through-dose exposures printed near best focus, it is common practice to print several through-dose exposure sets on one wafer, adjusting the height of the wafer between each set. At the Berkeley facility the focus steps are typically on the order of 50 nm. Assuming that nominal focus is somewhere in the FEM, the random variable associated with aerial image defocus of the best-focus row in the FEM is uniform on the interval [-25, 25] nm with a standard deviation of ≈ 14 nm.

In practice, it is sometimes difficult to decide which row in the FEM is truly at best focus. Focus drifts through dose are periodically found to shift the best focus row by one step from the lowest to highest doses. Often times the true focus of the exposure tool is right between focus steps of the wafer, causing neighboring rows in the FEM to print almost identical through-dose data sets. Even for the most experienced persons, determining the best-focus row is routinely somewhat subjective.

A potential issue with the contact-hole metric is that it assumes the experimental data is from the best-focus row in the FEM. If the experimental data is taken from one row above or below the best-focus row of the FEM, the random variable associated with aerial image defocus of the experimental set is uniform on the interval [75, 25] nm or [-25, -75] nm, respectively. One would expect that this level of defocus could alter the result of a resolution extraction when comparing the experimental data to modeled data generated with 0 nm of defocus.

Figure 1 shows SEM images of printed contact-holes through-dose at neighboring focus steps separated by 50 nm in two resists; the relative dose step between images is 1.32 in both resists. The rows labeled 'best' in each figure are considered by the authors to be in the best focus. This determination has been made by looking at printing characteristics at the lowest and highest doses. For doses that print well below the coded feature size, the best-focus row generally has contacts with the cleanest edges and the least PD variation. At doses that print well above the coded feature size, the astigmatism of the SEMATECH Berkeley exposure tool[13] gives rise to shape changes in printed contacts at high doses, flattening them slightly in the horizontal and vertical directions on either side of best focus.

The through-dose contact-hole sets in Figure 1 have been analyzed and resolution numbers have been extracted. The results are summarized in Table 1; we also show the results of another resist, resist H, although the corresponding SEM images are not included in the text. As expected, resists B and H show increases in reported blur on either side of best focus. For both of these resists the increase in extracted blur is on the order of the

[†]We define dose-to-size as the dose where features print at their coded dimension (their size on the mask multiplied by the tool magnification) at best focus.

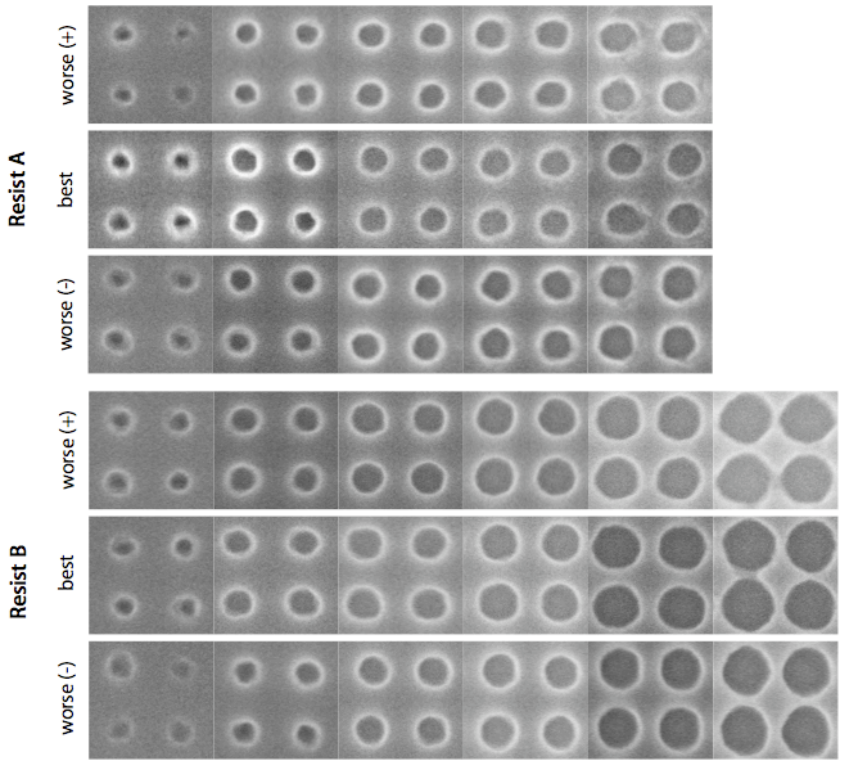

Figure 1. Through-dose SEM images of coded 1:1.5 50-nm dark-field contact-holes printed in resists A (top) and B (bottom) at three focus steps separated by 50 nm each. The relative dose step between SEM images is 1.32. The rows labeled 'best' are considered by the authors to be in the best focus.

1.23 nm RMS error-bars reported in previous work.[9] For resist A, however, we observe a 2 nm drop in extracted resolution in the defocused 'worse+' data set as compared to the 'best' data set. Perhaps the explanation is that the 'worse+' data is in fact the best focus data set and the authors made an incorrect call. Unfortunately we do not have another set of through-focus data on resist A for direct comparison.

Overall the metric proves to be robust even with the ambiguity in experimental data selection. The average of the variances in extracted resolution of each through-focus data set is 1.16 nm, indicating that error-bars associated with determining the best-focus row in the FEM are on the same order as the error-bars associated with aerial image modeling limitations.[9] For resist formulations with small resolutions (i.e., resist A) these data show that cross-platform comparisons could benefit from repeated experimental trials to reduce the measurement uncertainty through statistical averaging.

Table 1. Focus dependence on extracted resolution.

Focus[a]	Resist A	Resist B	Resist H
worse +	7.73 (1.33)	21.56 (1.68)	12.51 (1.20)
best	9.90 (0.28)	20.50 (0.44)	11.53 (1.32)
worse −	10.39 (0.99)	22.70 (1.32)	12.33 (0.95)

[a] The focus definitions used here are consistent with those in Figure 1.

4. SEM IMAGE EDGE-DETECTION THRESHOLD

Once images are captured with the SEM they are analyzed using offline image analysis software to measure PD at a given intensity threshold. As one can imagine, changing the predefined threshold alters the result of the

measurement. Table 2 shows the measured PD's for a through-dose set of SEM images at 5 different programmed threshold levels along with the extracted resolution for each threshold level. We observe no significant change in extracted resolution throughout the range of thresholds we have studied. These data suggest that the contact-hole metric is relatively immune to changes in edge-detection schemes, however, cross-platform comparisons should make an effort to be as consistent as possible with image analysis methods.

Table 2. Extracted resolution dependence on edge-detection threshold.

Threshold	Measured PD through dose [nm]								Resolution [nm]
0.40	41.8	48.4	53.1	57.5	63.1	67.2	72.3	81.7	13.91
0.45	43.0	49.8	54.3	58.6	64.4	68.5	73.6	83.1	13.91
0.50	44.2	51.0	55.5	59.9	65.6	69.6	74.9	84.4	13.91
0.55	45.4	52.1	56.6	61.0	66.7	70.7	76.0	85.7	13.99
0.60	46.4	53.2	57.5	62.1	67.8	71.8	77.1	86.1	14.24

5. SEM ELECTRON BEAM DOSING

The complex phenomena of resist charging during a SEM measurement has been well-documented in the literature.[14,15] It has been shown that resist charge accumulation can lead to unwanted electron beam deflection that alters the result of a SEM linewidth measurement. In addition, there have been several reports suggesting that carbon deposition during SEM measurements can noticeably affect the result of a linewidth measurement.[16,17] To investigate the sensitivity of the contact-hole metric to these phenomena inherently associated SEM metrology, we have captured time-sequential SEM images of contact-holes in two resists. Figure 2 shows the time evolution of the measured PD during continuous electron beam exposure in two resists. Each resist has been imaged at two emission current settings; all other SEM parameters remain fixed. We point out that the imaged dose is different in each resist; resist D is imaged at a dose near dose-to-size and Resist C is imaged at an overdosed dose.

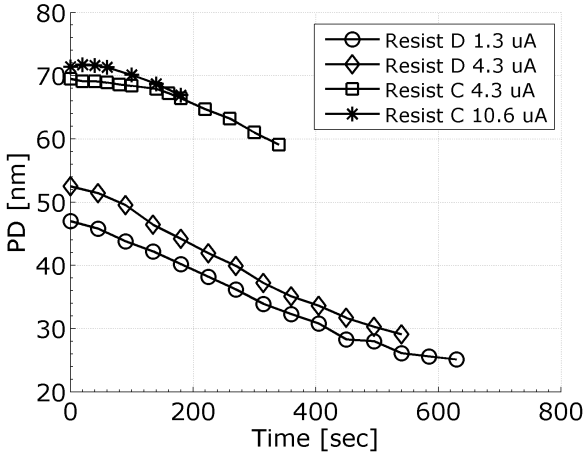

Figure 2. Measured PD as function of SEM exposure time in resists C and D; two SEM emission current settings are shown for each resist.

These data show that the measured PD evolves in both resists as the electron beam dose increases. After the two-minute mark, both resists show the same linear drop-off in measured PD with exposure time. Initially, however, each resist behaves a bit differently. At the 4.3 μA current setting, resist C is initially resistant to electron beam exposure showing less than 1 nm reduction in average PD in the first 120 seconds. Resist D, however, shows more than 6 nm PD reduction at the same current setting. In resist C the 10.6 μA current setting is noticeably different than the 4.3μA setting in terms of PD time-evolution. While the 4.3 μA setting

has a stable and slow initial PD reductuion, the 10.6 μA setting shows an increase in PD followed by a quicker roll-off to the steady-state rate. In resist D the changes in SEM emission current are less noticeable; the lower 1.3 μA setting has a slightly lower (4 nm) PD drop in the first 120 seconds and the roll-off trends for both emission currents are very similar. Unfortunately, we do not have 10.6 μA data for resist D for direct comparison.

In both resists we've noticed that increasing SEM emission current changes the measured PD. We believe this effect is the result of an increased signal-to-noise ratio that sharpens the edges of the contact wall in the captured image, changing the line-outs as seen by the image analysis software. We suspect, however, that this effect will not noticeably change extracted resolution as it should be consistent throughout all images within a through-dose set provided the emission current remains fixed. That said, this work shows that it is important to maintain the same emission current throughout each through-dose set of images[‡]. In terms of SEM electron beam dosing, the observed differences between PD time-evolution in resists C and D suggest that care should be taken to avoid premature exposure to the electron beam in the desired image area as it affects different resists in different ways and will reduce the credibility of cross-platform comparisons.

6. SEM FOCUS

There are many factors that affect the quality of an image captured in a SEM.[18] Assuming that the SEM is well-aligned and is properly corrected for stigma, perhaps the two biggest factors affecting image quality are signal-to-noise ratio and electron beam focus. Figure 3 shows through-SEM-focus images of coded 1:1.5 50 nm contacts printed at a dose slightly larger than dose-to-size. The images we show at each SEM focus are subsets of larger raw images containing > 28 contacts each; reported PD values are the average and variance (1σ) of 20 central contacts in each original image. To avoid SEM electron beam dosing between image captures a different (neighboring) part of the field is imaged at each SEM focus. For calibration purposes we also image seven neighboring field sites at the middle SEM focus and perform a field uniformity test. We find that average and variance of PD_{avg} are 60.9 and 0.98 nm, respectively, indicating that the ≈ 5 nm shift in measured PD through SEM focus is real.

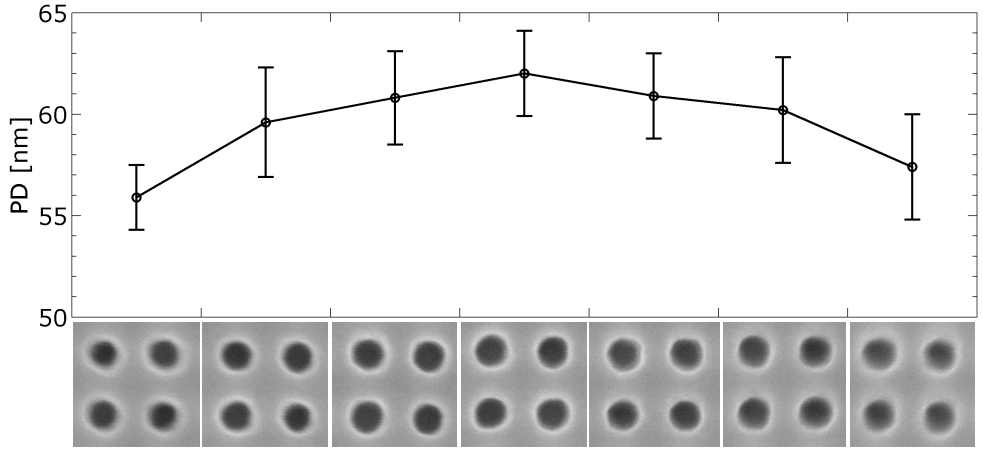

Figure 3. Measured printed diameter (PD) of coded 1:1.5 50 nm dark-field contact holes as a function of scanning electron microscope (SEM) focus. The plotted values are the average and standard deviation (1σ) of 25 neighboring contacts. To avoid SEM electron beam dosing between image captures a different part of the field is imaged at each SEM focus.

Ultimately we are interested in how SEM focus affects the result of a resolution extraction. We have imaged a through-dose set of contacts at three levels of deliberate SEM defocus; Figure 4 shows subsets of each through-dose set. Each set of data has been analyzed and curve-fit in the manner described in Sec 2 to extract a resolution number. The extracted resolutions for best, worse, and worst SEM focus as defined in Figure 4 are 11.31, 12.45 and 17.66 nm, respectively.

[‡]We have found that manually controlling the brightness knob on the SEM enables the through-dose set to be captured at one emission current setting while maintaining a reasonable dynamic range throughout the series of images.

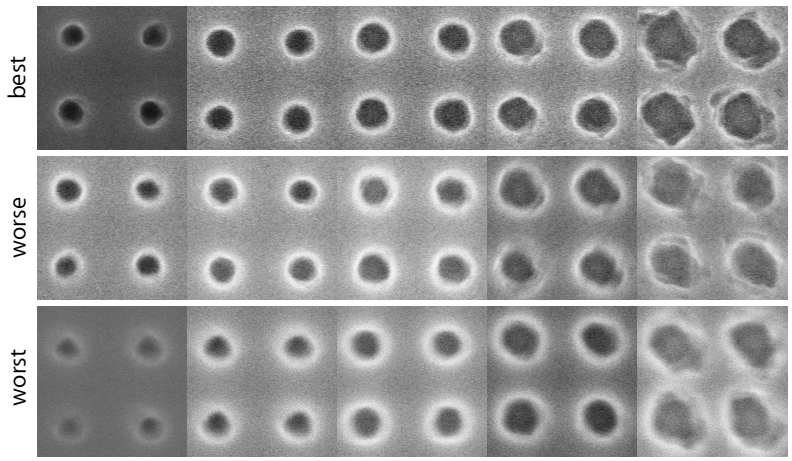

Figure 4. Through-dose images of coded 1:1.5 50 nm dark-field contact-holes at three levels of deliberate scanning electron microscope (SEM) defocus. The top row is well-focused and defocus increases in the downward direction. To avoid SEM electron beam dosing between image captures neighboring parts of the field are imaged at each SEM focus. Relative dose steps between images are 1.32.

Due to proximity effects in the convolution process that generate the defocused SEM image, SEM defocus causes larger absolute changes in measured PD (with respect to the measured PD at best SEM focus) for smaller contacts than it does for larger ones. This effect steepens the overall slope of the PD vs. dose curve. In addition, different levels of SEM defocus produce different dose-to-size values that in turn reshape the PD vs. dose curves differently during dose normalization. The combination of these two effects gives rise to significant changes in the PD vs. relative dose curves through SEM focus. This work shows that careful attention must be paid to ensure that well-focused SEM images are consistently captured. The authors would like to point out, however, that the observable defocus between the 'best' and 'worse' cases of SEM focus as defined in Figure 4 only shifts the extracted resolution by 1.14 nm; an amount equal to the magnitude of the previously reported error bars for the contact-hole metric.[9]

7. REPRODUCIBILITY

The SEMATECH Berkeley MET printing facility is known for it's long-term stability in terms of illumination conditions, optical aberrations, and focus control.[12] Here we examine the the reproducibility of the contact-hole metric by repeating identical experiments on different days for several resists. For a given resist formulation, the base coat, resist thickness, post-application bake, post-exposure bake, and illumination conditions remain fixed throughout the experiments. We do note, however, that different bottles of the same resist formulation have been used in two of the cases we present (resists E and G). In each repeated trial we have made every effort to ensure SEM images are in focus, with emission current fixed throughout each through-dose set. SEM electron beam dosing is avoided by focusing in on a local contact site and shifting the field by 1 μm just before image capture. All SEM images are captured by the same person. All PD measurements are made at the same programmed threshold level (0.5) in the image analysis software.

Table 3 shows the result of resolution extraction for the repeated experiments. In all three resists, the maximum resolution shift w.r.t. the average of the measurement trials is less than the 1.23 nm RMS error-bars that have been previously reported.[9] These data demonstrate that the error-bars discussed here and in previous work are representative of what we find in practice.

8. SUMMARY

In this paper we have examined the sensitivity of the contact-hole resolution metric to several sources of error associated with the experimental side of the resolution extraction process. This work has shown that for EUV exposures at the SEMATECH Berkeley MET printing facility, the contact metric has experimental sources of

Table 3. Reproducibility of the contact-hole resolution metric.

Resist E	Resist F	Resist G
22.14	16.71	26.56
20.50	16.24	25.46*
20.88*		
Exposure dates		
12-04-2007	10-25-2007	09-30-2006
12-05-2007	10-26-2007	04-06-2007*
09-07-2007*		

*Resist is from a different resist bottle than the above result(s).

error that are on the same order as the 1.23 nm RMS error-bars associated with modeling limitations.[9] Adding the experimental and modeling error-bars in quadrature we determine the full-process error-bar of the contact metric to be 1.75 nm RMS. The results of the reproducibility study support this conclusion. In repeated trials of resolution extraction for three different resists we find the shift in extracted resolution between trials is at most 1.64 nm (resist E) and is on average only about 1 nm. The experimental integrity of the contact-hole metric, combined with its low overhead in terms of modeling support and SEM images,[9] make it an attractive platform for resolution characterization.

ACKNOWLEDGMENTS

The authors are greatly indebted to Paul Denham, Ken Goldberg, Brian Hoef, Gideon Jones, and Jerrin Chiu of the Center for X-Ray Optics at Lawrence Berkeley National Laboratory for expert support with the exposure tool as well as the entire CXRO engineering team for building and maintaining the EUV exposure tool. We also acknowledge Tom Wallow, Robert Brainard, and Kim Dean for their support throughout this work. The authors are grateful for support from the NSF EUV Engineering Research Center. This research was also supported by SEMATECH and performed at Lawrence Berkeley National Laboratory using the SEMATECH MET exposure facility at the Advanced Light Source. Lawrence Berkeley National Laboratory is operated under the auspices of the Director, Office of Science, Office of Basic Energy Science, of the US Department of Energy.

REFERENCES

[1] H. Meiling, et. al, "First performance results of the ASML alpha demo tool," Proc. SPIE 6151, (2006).

[2] M. Miura, K. Murakami, K. Suzuki, Y. Kohama, Y. Ohkubo, T. Asami, "Nikon EUVL development progress summary," Proc. SPIE 6151, (2006).

[3] Stefan Wurm, "EUV Lithography Development in the United States" presented at the 4th International EUVL Symposium Steering Committee, San Diego, CA, November 7-9, 2005, proceedings available from SEMATECH, Austin, TX. (2005)

[4] B. Wu and A. Kumar, "Extreme ultraviolet lithography: A review," J. Vac. Sci. Technol., B 25(6), Nov/Dec (2007).

[5] G. M. Schmid, M. D. Stewart, C. Wang, B. D. Vogt, M. Vivek, E. K. Lin, C G Willson, "Resolution limitations in chemically amplified photoresist systems," Proc. SPIE 5376, 333-342 (2004).

[6] G. F. Lorusso, P. Leunissen, M. Ercken, C Delvaux, F.V. Roey, N. Vandenbroeck, "Spectral analysis of line width roughness and its applications to immersion lithography," J. Microlith., Microfab., Microsyst., 5(2) (2006).

[7] J. Hoffnagle, W. D. Hinsberg, F. A. Houle, and M. I. Sanchez, "Characterization of photoresist spatial resolution by interferometric lithography", Proc. SPIE 5038, 464-472 (2003).

[8] T. Brunner, C. Fonseca, N. Seong, M. Burkhardt, "Impact of resist blur on MEF, OPC and PD control," Proc. SPIE 5377, (2004)

[9] C. Anderson and P. Naulleau, "Sensitivity study of two high-throughput resolution metrics for photoresists," Appl. Opt. Vol 47, No. 1 (2008).

[10] P. Naulleau and C. Anderson "Lithographic metrics for the determination of intrinsic resolution limits in EUV resists," Proc. SPIE 6517, (2007)

[11] C. Ahn, H. Kim, and K. Baik, "A novel approximate model for resist process," Proc. SPIE 3334, 752763 (1998).

[12] P. Naulleau "Status of EUV micro-exposure capabilities at the ALS using the 0.3-NA MET optic," Proc. SPIE 5374, 881-891 (2004).

[13] P. Naulleau, C. Anderson, K. Dean, P. Denham, K. Goldberg, B. Hoef, B. La Fontaine, T. Wallow, "Recent results from the Berkeley 0.3-NA EUV microfield exposure tool," Proc SPIE 6517, (2007).

[14] K. M. Monaham, J. P. H. Benschop, and T. A. Harris, "Charging effects in low-voltage SEM metrology," Proc. SPIE 1464, 2-9 (1991).

[15] M. Davidson and N. T. Sullivan, "An investigation of the effects of charging in SEM based CD metrology," Proc. SPIE 3050, 226-242 (1997).

[16] T. W. Reilly, "Metrology algorithms for machine matching in different CD SEM configurations," Proc. SPIE 1673, 48-55 (1992).

[17] K. Phan, J. Nistler, B. Singh, "Metrology issues associated with submicron linewidths," Proc. SPIE 1464, 424-437 (1991).

[18] H. J. Levinson *Principles of Lithography,* 2^{nd} *Edition* Ch. 9, SPIE Press, Bellingham, WA (2005).